

Chemomechanical coupling of the forward and backward steps of single kinesin molecules

Masayoshi Nishiyama*†‡, Hideo Higuchi§¶†† and Toshio Yanagida*##**

*Single Molecule Processes Project, ICORP, JST, 2-4-14, Senba-Higashi, Mino, Osaka, 562-0035, Japan

†Department of Biophysical Engineering, Osaka University 1-3, Machikaneyama, Toyonaka, Osaka, 560-8531, Japan

§Department of Metallurgy, Graduate School of Engineering, Tohoku University, Sendai, 980-8579, Japan

¶Center of Interdisciplinary Research, Tohoku University, Sendai, 980-8579, Japan

#Department of Physiology and Biosignaling, Graduate School of Medicine, Osaka University, 2-2, Yamadaoka, Suita, Osaka, 565-0871, Japan

**Laboratories for Nanobiology, Graduate School of Frontier Biosciences Osaka University, A4, 2-2 Yamadaoka, Suita, Osaka, 565-0871, Japan

‡Current address: Department of Chemistry, Graduate School of Science, Kyoto University, Kyoto, 606-8502, Japan

††e-mail: higuchi@material.tohoku.ac.jp

Published online: 23 September 2002; doi 10.1038/ncb857

The molecular motor kinesin travels processively along a microtubule in a stepwise manner. Here we have studied the chemomechanical coupling of the hydrolysis of ATP to the mechanical work of kinesin by analysing the individual stepwise movements according to the directionality of the movements. Kinesin molecules move primarily in the forward direction and only occasionally in the backward direction. The hydrolysis of a single ATP molecule is coupled to either the forward or the backward movement. This bidirectional movement is well described by a model of Brownian motion assuming an asymmetric potential of activation energy. Thus, the stepwise movement along the microtubule is most probably due to Brownian motion that is biased towards the forward direction by chemical energy stored in ATP molecules.

Kinesin is a molecular motor that moves processively along a microtubule^{1–5} with regular 8-nm steps^{6–9}. Kinesin moves primarily in the forward direction (to the plus end of the microtubule) and occasionally in the backward direction (to its minus end), which has been commonly called a back step^{10–13}. The maximum force against which single kinesin molecules work is 7 pN (refs 13–15).

To understand the mechanical properties of this mechanoenzyme, the relationship between force and sliding velocity has been

investigated from averaged time courses of movement^{10–16}. In previous studies, the back steps were included in the individual traces but were ignored in the analysis because they were considered to be rare events compared with the regular 8-nm steps in the forward direction.

The mechanism underlying these forward and backward movements remains unclear. Here we have characterized the stepping mechanism by correlating both the forward and the backward movements of single kinesin molecules to the hydrolysis of ATP.

Table 1 Rate constants of the branched kinetics

Force (pN)	Energy difference of the barriers* (k _B T)	Rate constants†				Velocity§ (nm s ⁻¹)	Run length¶ (nm)
		k ₁ (μM ⁻¹ s ⁻¹)	k ₂ (s ⁻¹)	k _{3f} (s ⁻¹)	k _{3b} (s ⁻¹)		
0	5.4	3.4	140	770	3.5	930	3600
3.8	2.6	1.4	140	47	3.1	230	200
7.6	0	0.21	140	2.9	2.9	0	0

The parameters were calculated from the analysis of the dwell time for each force.

*Energy difference = 5.4k_BT - F × 2.9[nm].

†k₁ = k_{cat}/K_m, k_{cat} = k₂(k_{3f} + k_{3b})/(k₂ + k_{3f} + k_{3b}), k₂ = 1/τ₂, k_{3f} = R₀exp(-Fd₁/k_BT)/(R₀+1)/τ₃, k_{3b} = exp(-Fd₂/k_BT)/(R₀+1)/τ₃, K_m = 36 μM (0 pN) and 27 μM (3.8 and 7.6 pN), τ₂ = 7.0 ms, τ₃ = 1.3 ms, R₀ = 221, d₁ = 3.0 nm, d₂ = 0.1 nm.

§Velocity = 8[nm] × ε × k_{cat} [s⁻¹], ε = P_f - P_b = (k_{3f}/k_{3b} - 1)/(k_{3f}/k_{3b} + 1)

¶Run length = 8[nm] × (2P_f/P_b) × ε. The number of the stepwise movements until detachment occurred is described as 2P_f/P_b, because the ratio of the detachment is roughly half the total number of movements in the backward direction. The ratio of detachment in total backward movement may be due to the experimental system.

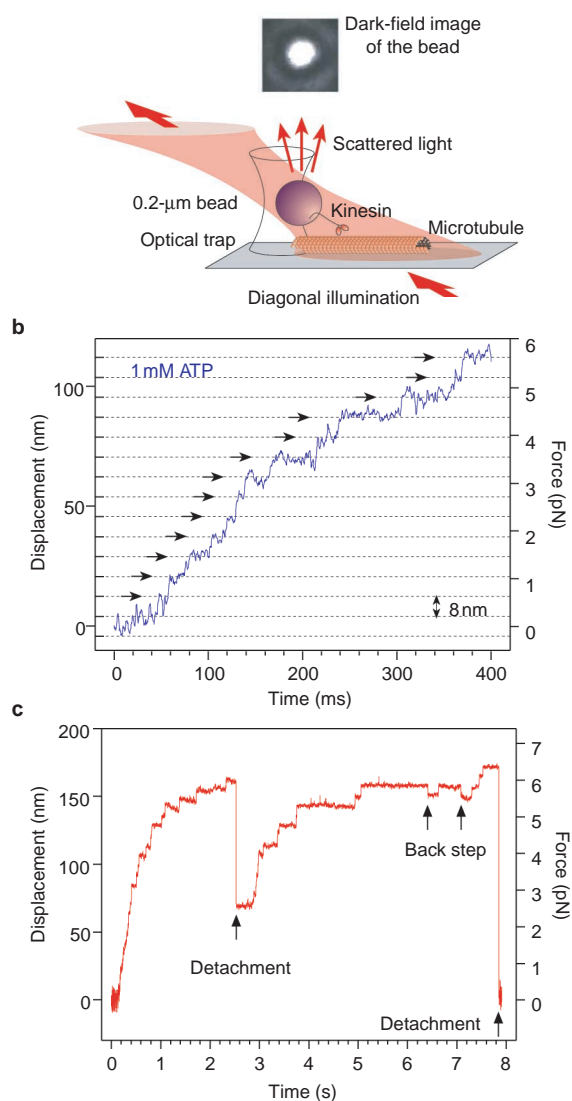


Figure 1 Nanometry of single kinesin molecules. **a**, The optical trapping nanometry system (not to scale). **b**, **c**, Time courses of the displacements of single kinesin molecules. The ATP concentration was 1 mM (**b**) and 10 μ M (**c**). The displacement of kinesin was obtained from the bead displacement with the compliance of the experimental system (Methods). The force was calculated from the bead displacement and the trap stiffness (0.05 pN nm⁻¹ in **b**; right axis).

Results

Stepwise movements of single kinesin molecules. Single kinesin molecules were attached to a bead captured by an optical trap and brought into contact with a microtubule attached to a glass surface (Fig. 1a). The bead was illuminated diagonally by a focused red laser and its dark field image was projected onto a quadrant photodiode. The displacement of the bead was determined by measuring the differential output of the quadrant photodiode with nanometer accuracy¹⁷.

The time course of kinesin movement showed a distinctive stepwise pattern with regular 8-nm steps at forces greater than 0.5 pN; this regular step size is clearly indicated by the lines drawn at 8-nm intervals in Fig. 1b. Kinesin moved primarily in the forward direction but occasionally in the backward direction (Fig. 1c, arrows). We characterized these stepwise movements by analysing the force, step size and dwell time between the stepwise movements.

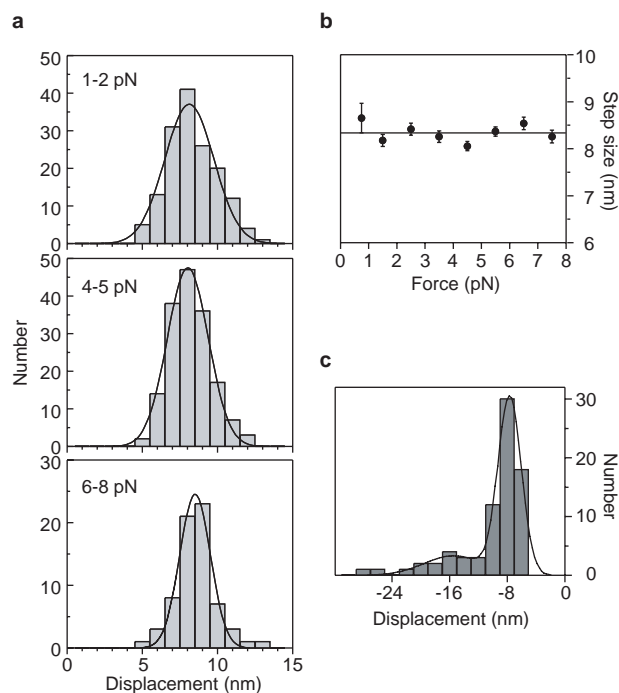


Figure 2 Step size of the forward and backward movements. **a**, Histograms of the step size at 10 μ M ATP and forces of 1–2, 4–5 and 6–8 pN. Lines are the best fits of the data to a gaussian curve; the peak position and width are 8.2 and 1.6 nm (1–2 pN), 8.1 and 1.1 nm (4–5 pN), and 8.4 and 0.9 nm (6–8 pN), respectively. **b**, Step size as a function of load. The step sizes (mean \pm s.e.m.) were obtained from the peak position in **a** at each load (ATP concentration 10 μ M, $n = 13$ –177, total = 937). The average step size at each load is 8.3 nm (line). **c**, Histogram for the step sizes of the back steps. Displacement data (<30 nm) at ATP concentrations of 1 mM and 10 μ M are included. The line is the sum of two gaussian peaks fitted to the data; the positions and widths of each peak are -7.7 and 1.6 nm, and -15.5 and 4.1 nm (twice the displacement at the main peak), respectively. The 16-nm step cannot be resolved into two 8-nm steps even at the submillisecond temporal resolution. It is likely that the 16-nm steps are induced in a single cycle of ATP hydrolysis, indicating that the back step may be due to the rebinding of kinesin to other sites of the microtubule after detachment.

The step size was determined directly from the distinctive pattern of movements in the time courses for kinesin (see Methods). For the forward steps, the step size was 8 nm and was independent of the load (Fig. 2a, b) and ATP concentration (8.0 and 8.3 nm at ATP concentrations of 1 mM and 10 μ M, respectively). For the back steps, the step size was either 8 nm or 16 nm (Fig. 2c) and was independent of the load and ATP concentration (data not shown).

We also tested whether other short steps existed in the dwell time between the 8-nm steps^{7,16,18,19}. Typical traces of the region between the adjacent 8-nm steps on an expanded timescale showed no evidence of short steps (Fig. 3a). To measure changes in displacement with greater accuracy, we averaged the traces after synchronizing the rising phases of the 8-nm steps at the start and end of the dwell time²⁰. The averaged traces did not show any significant displacements (>1 nm) in the dwell time at temporal resolution of 1 ms (Fig. 3b). Similar results were also obtained from analysis of the back steps (data not shown). Thus, kinesin moves only in 8-nm steps in the forward direction and in 8-nm and 16-nm steps in the backward direction, but not in steps shorter than 8 nm.

Directionality of the step. Kinesin moved primarily in the forward direction at low loads. The occurrence of back steps (step size <30 nm) and detachments (>30 nm) increased with the load

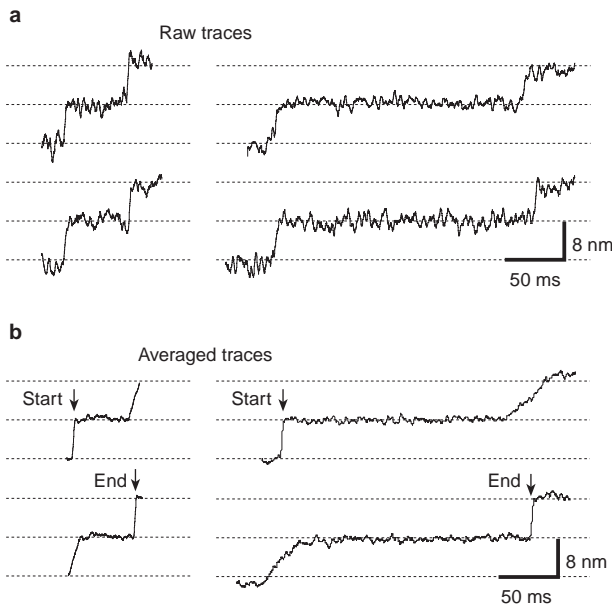


Figure 3 Displacements of kinesin in the dwell time. **a**, Raw traces of the stepwise displacements recorded with a bandwidth of 500 Hz. **b**, Traces averaged at the start and end step of the dwell time. The raw stepwise movements shown in **a** were collected from the time courses at forces of 1–7 pN (left, dwell time 50 ± 5 ms, $n = 37$; right, dwell time 200 ± 20 ms, $n = 15$). The top traces were obtained by averaging the individual time courses after synchronizing the 4-nm points of the 8-nm steps ('start' step, arrows). The accuracy of the averaging procedure was about 1 ms, which was verified by the rise time of the individual averaged traces (corresponding to the displacement from 1 nm to 7 nm). The bottom traces were obtained by averaging the traces at the 4-nm point of the 'end' step. The ATP concentration was $10 \mu\text{M}$ (**a** and **b**).

(Fig. 1c). We analysed the direction of movement by counting the number of 8-nm steps, back steps and detachments as a function of the load at 1-pN intervals from 0.5 pN to 8.5 pN at ATP concentrations of 1 mM and $10 \mu\text{M}$ (Fig. 4a). At loads lower than 4 pN the fraction of 8-nm steps was almost equal to 1, indicating that almost all steps were made in the forward direction. As the load increased, the fraction of the 8-nm steps gradually decreased.

Correspondingly, the occurrence of back steps and detachments increased with an increase in load. The sums of them are plotted as the 'backward movements' (dotted lines) with respect to the 'forward movements' (8-nm steps) in Fig. 4a. The fraction of backward movements increased exponentially with load and intersected with that of the forward movements at 7–8 pN.

We characterized the load dependence of the stepping direction by calculating the ratio of the forward to the backward movements at each load. The ratio decreased exponentially with load, and the plots of ratio against load in the presence of 1 mM and $10 \mu\text{M}$ ATP could almost be superimposed (Fig. 4b). These results show that the fraction of forward and backward movements is dependent on load but not on the concentration of ATP. Thus, the load modifies the stepping motion, resulting in unidirectional movements.

Dwell time. To relate the 8-nm steps, back steps and detachments to the kinetic pathway, we analysed the dwell time between the stepwise movements. The dwell time was directly measured from the movement time courses and averaged at each load and ATP concentration for the different types of stepwise movement (see Methods). Figure 5a shows the average dwell times before an 8-nm step at saturating (1 mM) and limiting ($10 \mu\text{M}$) concentrations of ATP. The dwell time increased with load and decreased with concentration of ATP. The relationship between force and dwell time at

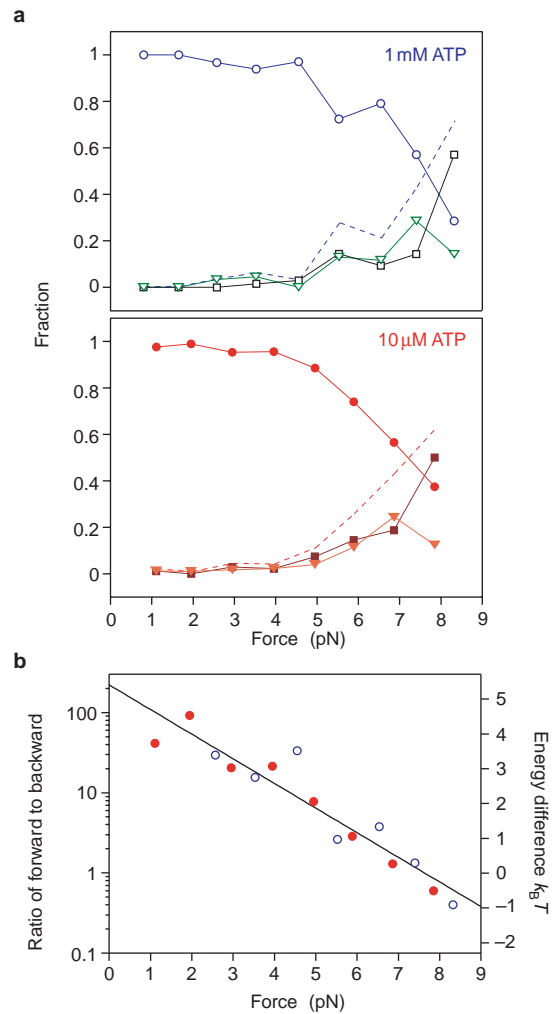


Figure 4 Step directionality. **a**, Fraction of 8-nm steps (circles), back steps (triangles) and detachments (squares) as a function of the force. Fractions were obtained from the number of 8-nm steps, back steps and detachments at each force in the presence of 1 mM ($n = 5-69$, total = 380) and $10 \mu\text{M}$ ATP ($n = 8-186$, total = 990). **b**, Ratio of the forward to backward movements. Data were obtained at 1 mM ATP (open circles) and $10 \mu\text{M}$ (filled circles). Data are not plotted for points where backward movements were not observed. The plots at 1 mM and $10 \mu\text{M}$ ATP were fitted to equation (1), with $R_0 = 221$ and $d = 2.9$ nm. The energy difference between the backward and forward direction barriers is shown on the right.

an ATP concentration of 1 mM, plotted on the log scale, deviated from a straight line (data not shown). This means that the relationship between force and dwell time cannot be described by a simple exponential curve. The dwell time at saturating ATP concentrations has been shown to comprise load-dependent and load-independent transitions^{21,22}. Taking into consideration the fact that the ATP binding reaction is limiting at low ATP concentrations, there are at least three transitions in a single dwell time.

Figure 5b summarizes the dwell time before the occurrence of back steps and detachments. Each plot is the average dwell time at each ATP concentration, obtained using the method used for the 8-nm steps. Notably, the dwell time of the back steps and detachments was altered by the load and the ATP concentration. The backward movements did not occur easily under high loads and limiting ATP concentrations, similar to that found for the forward

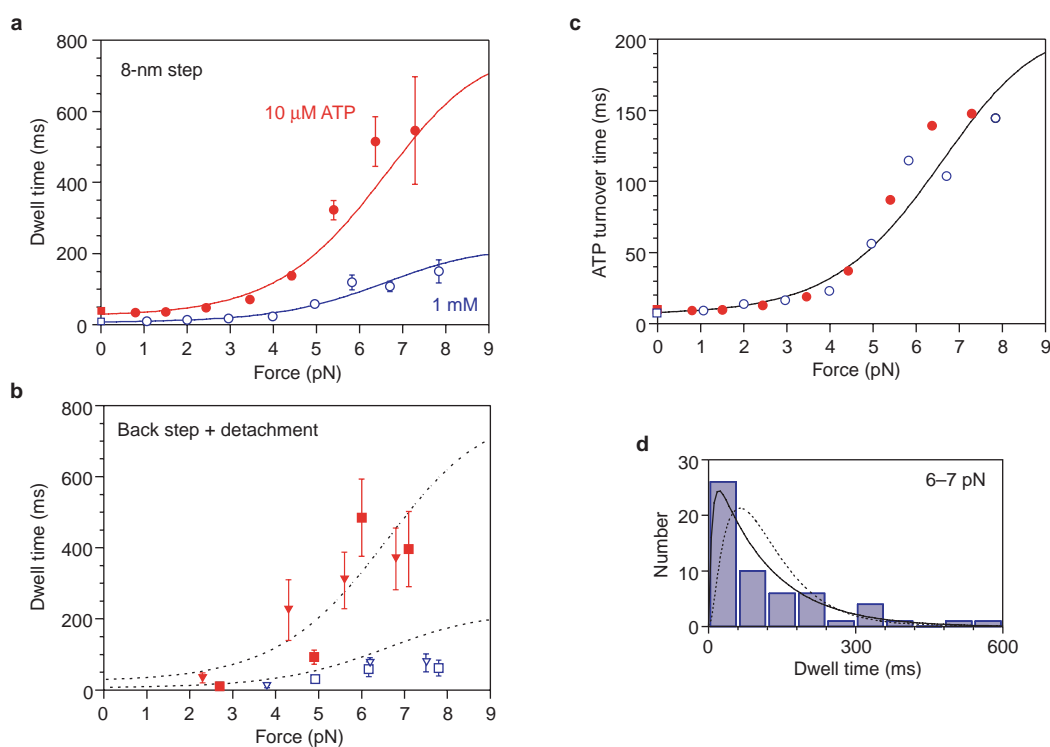


Figure 5 Dwell time between the adjacent stepwise movements. **a**, Dwell time before the 8-nm step as a function of force. Each point represents the average dwell time at ATP concentrations of 1 mM (open circles, $n = 21-64$, total = 327) and 10 μM (filled circles, $n = 13-177$, total 889). The curves were obtained from equations (3) and (6). **b**, Dwell time before the back step and detachment. Each plot is the average value of the dwell time at 1 mM ATP (back step (open triangles), $n = 8-9$, total = 25; detachment (open squares), $n = 9-10$, total = 28) and 10 μM ATP (back step (filled triangles), $n = 6-18$, total = 46; detachment (filled squares), $n = 6-23$, total = 63). The dotted curves represent the unbroken lines in **a** and are included for comparison. **c**, ATP turnover time was calculated from the dwell time in

a with equation (6) and $K_m = 27 \mu\text{M}$. Plots in the presence of 1 mM (open circles) and 10 μM (filled circles) ATP have been fitted by equation (3) with $\tau_2 = 7.0 \text{ ms}$, $\tau_3 = 1.3 \text{ ms}$ and $d_f = 3.0 \text{ nm}$. **d**, Histogram of the dwell time before an 8-nm step at 6–7 pN. The ATP concentration was 1 mM. The unbroken line is the fitting curve obtained from simulating the three-step reaction model shown in Fig. 6a with Lab VIEW v.5.1 (National Instruments)¹³. Three rate constants were calculated from the equations and parameters (Table 1). The broken line was obtained by simulating the futile hydrolysis model, in which a single dwell time corresponds to two cycles of the same three-step reactions (six-step reactions in total).

movements (Fig. 5a). In fact, the dwell time of the back steps and detachments could be essentially described by the curve fit used for the 8-nm steps (Fig. 5b, dotted lines, and see below). Thus, the forward and backward movements may be coupled to the same kinetic pathway for the hydrolysis of ATP molecules.

According to Michaelis–Menten kinetics, a single dwell time consists of the ATP binding and hydrolysis reactions. The former is characterized by the Michaelis constant, K_m , which in this case describes the affinity of kinesin for ATP. We calculated the K_m at each load from the ratio of the dwell time at 10 μM ATP to that at 1 mM ATP using equation (7) in Methods. The ratio was 3.8, 3.2 and 3.6 at 1, 3 and 5 pN, respectively (average ratio 3.7), and was therefore independent of the force. Thus, the K_m was 27 μM irrespective of the load, which enabled us to calculate the ATP turnover time. Figure 5c plots the relationship between force and ATP turnover time at ATP concentrations of 1 mM and 10 μM ; the two plots can be essentially described by the same curve (see below). Our results indicate that the ATP binding reaction for kinesin is independent of the load, which differs from the results of previous studies^{15,16}. This discrepancy might be due to the different approaches used for calculating the ATPase reaction: whereas we used the individual dwell time for the 8-nm steps, other studies used values obtained from averaged time traces^{15,16}. **Analysis of the bidirectional steps.** We incorporated the forward and backward movements into a three-state model with some modifications¹⁸. The three states of K, K.T and K.D considered in

the analysis correspond to kinesin with no bound nucleotide, with bound ATP and with bound ADP (or ADP.Pi), respectively (Fig. 6a). The forward (f) and backward (b) movements occur in parallel, such that the kinetic pathway branches at the K.D state. The rate constant from K.D to K is given as the sum of k_{3f} and k_{3b} . The ratio of the forward to backward movements is equal to k_{3f}/k_{3b} . According to Arrhenius/Eyring kinetics, the rate constant is related to the activation energy of the barrier potential. We therefore used an asymmetric potential to analyse the bidirectional stepwise movements.

The activation energy of the forward and backward directions can be described by $E_f + Fd_f$ and $E_b + Fd_b$, respectively, where E_f and E_b are the heights of the barrier maximum at zero load, and d_f and d_b are the characteristic distances against the load F (Fig. 6b). If the Boltzmann energy distribution is assumed, then the rates in the forward and backward direction will be proportional to $\exp[-(E_f + Fd_f)/k_B T]$ and $\exp[-(E_b + Fd_b)/k_B T]$, respectively²¹, where k_B is the Boltzmann constant and T is the experimental temperature (298 K). The number of forward movements relative to the backward is equal to k_{3f}/k_{3b} under kinetic control and is given by:

$$k_{3f}/k_{3b} = R_0 \exp(-Fd/k_B T) \tag{1}$$

$$d = d_f - d_b \tag{2}$$

where $R_0 = \exp[(E_b - E_f)/k_B T]$ is the ratio of the rate constants at no

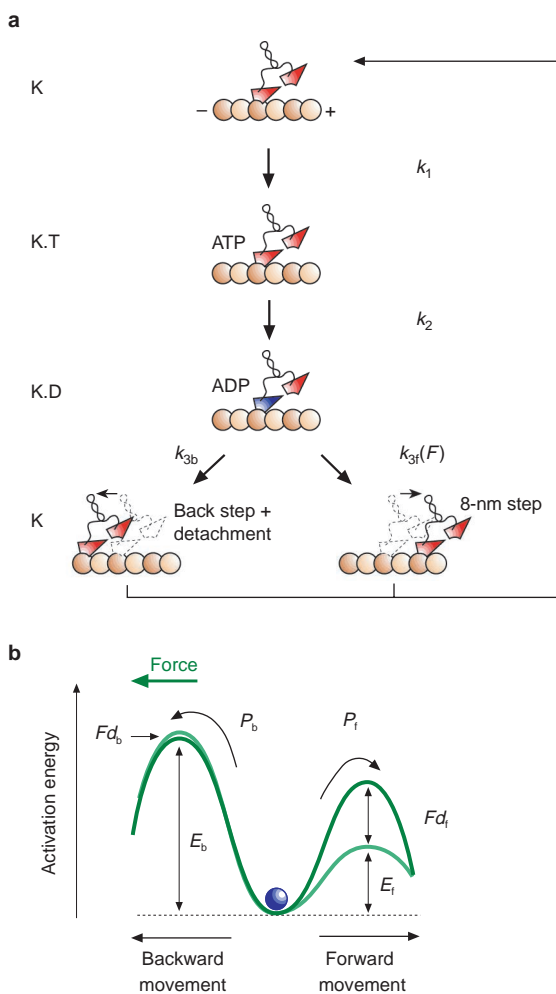


Figure 6 **Stepping kinetics of the bidirectional movements.** **a**, Branched kinetic pathway. Kinesin attached to the microtubule with one motor domain (state K). The ATP molecule binds to the head (state K.T) and is hydrolysed (state K.D). After kinesin moves either to the forward or backward direction, the ADP molecules are released (state K). **b**, Asymmetric potential of the activation energy (see text).

load and d is the difference of the characteristic distances. The plots in Fig. 4b were fitted by equation (1), with $R_0 = 221$ and $d = 2.9$ nm. The energy difference between the backward and forward direction barrier maximums was $5.4 k_B T$ at zero load, and the difference decreased linearly with load. When the load reached 7.6 pN, the barrier height of the forward direction was equal to that of the backward direction, and the directionality of the motion disappeared. Thus, the stall force could be determined as the force at which the probabilities of the forward and backward movements were equal.

According to our branched three-state model, the ATP turnover time, τ_{cat} is composed of the inverse of k_2 and the inverse of $k_{3f} + k_{3b}$. Thus, τ_{cat} is given by:

$$\tau_{cat} = \tau_2 + \tau_3 \cdot \left\{ \left(\frac{R_0}{R_0 + 1} \right) e^{-F d_f / k_B T} + \left(\frac{1}{R_0 + 1} \right) e^{-F (d_f - d) / k_B T} \right\}^{-1} \quad (3)$$

where τ_2 is $1/k_2$ and is independent of the load, and τ_3 is $1/(k_{3f} + k_{3b})$ in the absence of a load^{21,22}. The ATP turnover time at

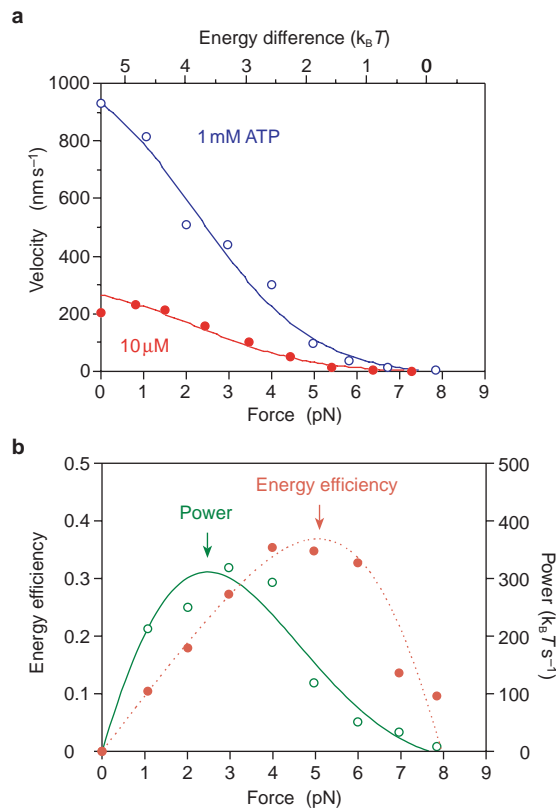


Figure 7 **Mechanics and energetics.** The stepping efficiency is $\alpha(F) = P_f - P_b$, where P_f and P_b are the probabilities of the forward and backward movements ($P_f + P_b = 1$), respectively, and F is the force. Each ATP hydrolysis reaction is assumed to result in a stepwise movement. The step size of the backward movement has been standardized to 8 nm. **a**, Force-velocity relationships. Velocities in the presence of 1 mM (open circles) and 10 μ M (filled circles) ATP were calculated as $L e / \tau$, where L is the step size of 8 nm and τ is the average dwell time. When the force-velocity relation is normalized to zero load levels, the velocity is no longer dependent on the ATP concentration. The energy difference between the backward and forward direction barriers is shown on the top axis. **b**, Energy efficiency and power. Work is defined as $W = L F e$. The energy efficiency, E , and power, P , at an ATP concentration of 1 mM were obtained from $E = W / (20 k_B T)$ (filled circles and dotted line; left axis) and $P = W / \tau$ (open circles and unbroken line; right axis).

ATP concentrations of 1 mM and 10 μ M (Fig. 5c) could be well fitted by equation (3), with $\tau_2 = 7.0$ ms, $\tau_3 = 1.3$ ms and $d_f = 3.0$ nm. In addition, d_b was calculated to be 0.1 nm by equation (2). The small value of d_b indicates that the backward barrier height is not greatly altered by the effect of a load. Table 1 shows the summary of the rate constants at 0, 3.8 and 7.6 pN (the stall force), which is consistent with previous studies using either a single-molecule assay^{8,13} or steady-state kinetics^{23,24}. Thus, load dependence of the dwell time can be mainly ascribed to the rate constant of k_{3f} .

In the above discussion, we assumed that each cycle of the ATP hydrolysis reaction is coupled to a stepwise movement. This assumption has been confirmed at low loads^{9,15,25} but not at high loads. We therefore characterized the chemomechanical coupling at high loads by studying the possibility of ‘futile hydrolysis’^{15,16} — that is, the possibility that ATP is hydrolysed but kinesin fails to generate the movement. The histogram of the dwell time before an 8-nm step at 6–7 pN shows a monotonic decrease (Fig. 5d), consistent with our model in which the kinetic pathway has one rate limiting reaction at high loads and saturating ATP concentrations. If the futile hydrolysis reactions occur frequently at high loads, then the result would be a large shift in the position of peaks or the

occurrence of the additional peaks. Such changes were not apparent in Fig. 5d.

We next determined the number of ATP molecules consumed at each stepwise movement by trying to fit the dwell time histogram with curves corresponding to simple hypotheses^{25,26}. The histogram could be fitted to the curve by assuming that one ATP molecule is always consumed per stepwise movement (unbroken line, reduced $\chi^2 = 1.1$), but not by assuming that two ATP molecules were consumed per stepwise movement (broken line, reduced $\chi^2 = 5.6$). Thus, the latter hypothesis was rejected at a significance of less than 1% using the χ^2 -test. Similar results were obtained from the dwell time histogram at other force levels. Therefore, futile hydrolysis reactions do not occur frequently even at high loads, indicating that the hydrolysis reaction of ATP molecules for kinesin most probably results in a stepwise movement.

Mechanics and energetics of the stepwise movements. We characterized the mechanical and energetic aspects of the bidirectional movements of kinesin by calculating the velocity, run length, energy efficiency per ATP turnover and power. Our calculations using data from individual steps enabled us to compare our results with previous values obtained from averaged traces.

Figure 7a shows the force–velocity curves of the stepwise movements; these did not show linear^{10–14} or upper concave^{15,16} relationships, as found in previous studies, but were more similar to the inverse proportion²⁷. This discrepancy is most probably due to the different methods used for calculating the velocity, that is, individual stepwise movements (used here) versus those obtained from averaged traces^{10–16}. We estimated the run length of kinesin along a microtubule from the stepping efficiency (Table 1). The run length at zero load was about 3 μm , which is reasonably consistent with previous values^{2–4,14,28}. When a load was applied to kinesin, the run length decreased exponentially with the increment of the load¹⁶ and reached zero at 7.6 pN (Table 1). We characterized the energetic aspects of the bidirectional movement by the energy efficiency and power, which we calculated from the work taking into account the stepping efficiency (Fig. 7b). The energy efficiency and power showed peaks at moderate loads, but these peaks had different positions. Notably, similar results have been reported for studies using muscle fibres²⁷.

Discussion

We have analysed the individual stepwise movements — that is, the 8-nm steps, back steps (<30 nm) and detachments (>30 nm) — of kinesin travelling along microtubules. It seems that the hydrolysis of single ATP molecules can be coupled to either the forward or the backward movement. This indicates that the chemomechanical coupling is not deterministic. Thus, kinesin may be a loosely coupled motor because the ATP hydrolysis reaction does not necessarily couple to the forward movement. How the forward and backward movements are created through hydrolysis of ATP is outlined below and in Fig. 6a.

In the absence of ATP, kinesin molecules attach to a microtubule through one head (rigor), leaving the other one free (refs 29, 30; state 'K'). ATP molecules bind to the head that is linked to the microtubule according to Michaelis–Menten kinetics (refs 2, 24; state 'K.T'). We obtained a Michaelis constant of 27 μM , and this value is independent of the load¹¹. Because the stepwise movements take place through a load-dependent transition (Fig. 4), kinesin is not able to move in the forward direction in the K.T state. The nucleotide hydrolysis process from ATP to ADP (state 'K.D') causes a structural change of the kinesin head^{31,32}, such that the binding between kinesin and the microtubule is changed to a highly mobile state^{33,34}.

The unidirectional movement of kinesin has never been reported in the presence of ADP, but no ATP; thus, the free energy released from ATP hydrolysis is essential for creating the 8-nm step. This energy may be stored in the ATP molecules^{16,35}, as demonstrated by

a load-dependent asymmetric potential (Fig. 6b). Kinesin in the energy-charged K.D state is able to make an 8-nm step, although there is also the risk of a back step or detachment. After the kinesin molecule moves to the next binding site, the ADP molecule is released and the head returns to the immobile state at the new binding site (state 'K'). This rapid dissociation might be involved in inhibiting any additional movements, such that kinesin makes only a single stepwise movement at each hydrolysis of ATP.

The load dependence of the stepwise movements is characterized primarily by the large characteristic distance, $d_t = 3.0$ nm, which indicates the existence of substeps^{16,18}. In our experiments, however, analysis in the millisecond time range showed no evidence of steps shorter than 8 nm (Figs 2 and 3). Thus, the most likely explanation is that the substep coincides with the rising phase of the 8-nm step. This has already been proved by measuring the nanometre displacements of kinesin with microsecond accuracy, showing that the 8-nm step is composed of sequential 4-nm substeps¹⁷. These rapid two-step reactions can be explained by a 'hand-over-hand' process, in which the two heads of kinesin work in a coordinated manner^{18,36}. A structural change in the motor domain initiates the partner head to attach to the next binding site, which is 8 nm from the initial binding site^{28,31}. The rear head then detaches from the initial binding site. In this mechanism, the role of each head would alternate at each ATPase cycle.

But it has been reported that single one-headed kinesin molecules can move processively along the microtubule^{37,38}. This indicates that the two-headed structure is not required for motility, because a stepwise movement can be achieved by single head. Thus, the role of the partner head might be to stabilize the kinesin–microtubule complex, similar to the K-loop of the KIF1 motor^{38,39} or to biotin-dependent transcarboxylase (BDTC) in single-headed kinesin³⁷, and assist in movements towards the plus end of the microtubule³¹. To move for a considerable distance, such as the length of the motor domain (7 nm), the head that is attached to the microtubule might step along the 4-nm repeat of tubulin monomers^{40,41} in a way that resembles hopping on one leg.

The stochastic behaviour of the forward and backward movements can be explained simply by a model of biased Brownian motion. Because Brownian motion is random, it must be biased in the forward direction to produce the unidirectional movement observed. In this study the forward and backward movements can be explained by the Brownian motion of a mass particle on a one-dimensional asymmetric potential of activation energy. According to the Arrhenius/Eyring kinetics, the asymmetry of the potential is ascribed to the different height of the barrier maximum; the energy difference is $5.4 k_B T$ (where $T = 298$ K) at zero load, which is about a quarter of the free energy of the ATP hydrolysis ($\sim 20 k_B T$).

Alternatively, another idea for the biased Brownian motion has been proposed on the basis of the thermal ratchet model^{42–44}. In this model, a simple motor consists of a ratchet and a pawl isolated at different temperatures that produces work and unidirectional motion. Two temperatures, T_f and T_b , control the probabilities of the forward and backward steps of motor molecules, respectively; in general, $T_f > T_b = T$ (the experimental temperature). In the thermal ratchet model, the probability of the forward movement but not the backward movement is dependent on the load. This is consistent with our results. Here, we calculated T_f from the ratio of the forward to the backward movement (Fig. 4b). We characterized an asymmetric potential assuming that the barrier height is E ($E = E_f = E_b$, regardless of the load) and the distance from the bottom to the forward barrier maximum is equal to the step size, thus, $d_f = 8$ and $d_b = 0$ nm. The experimental data were fitted by $T_f = 2.8 T$, leading to $T_f = 834$ K at the experimental temperature $T = 298$ K. The energy barrier in the potential was $8.4 k_B T$, which is roughly half of the free energy of the ATP hydrolysis.

We used these procedures to estimate the T_f of the other processive motor molecules — 22S dynein of *Tetrahymena* cilia⁴⁵, the inner-arm dynein c of *Chlamydomonas* flagella⁴⁶ and myosin V

(ref. 22) — from the ratio of the step size to the characteristic distance. Notably, the T_f of these motors is about $3T$ (~ 900 K), which is almost the same as that of kinesin. Thus, the ATP-driven processive motors, kinesin, dynein and myosin, would seem to be programmed to work with the same chemomechanical energy transduction mechanism.

We conclude that the forward and backward movements of kinesin are created by a similar chemomechanical energy transduction mechanism. The stepwise movement is essentially Brownian motion that is biased in the forward direction. The biased Brownian motion is caused by the interaction between kinesin and the microtubule, which is dynamically changed by the free energy derived from the hydrolysis of ATP. □

Methods

Single-molecule assays

We obtained kinesin and tubulin from bovine brains and purified them as described^{8,13}. Tubulin was labelled with tetramethylrhodamine succinimidyl ester and then polymerized into microtubules. We carried out single-molecule assays by using the improved optical trapping nanometry system¹⁷ with some modifications.

Kinesin was mixed with bead solution at a molar ratio of kinesin to beads of 0.5, so that the kinesin-coated beads moved onto the microtubule with a probability of 0.31. Taking the geometry of the kinesin on the bead into account^{10,13}, the probability that a single kinesin molecule would interact with a microtubule was 0.95. We discarded the results from beads with a maximum force of more than 9 pN, because it was thought that on these beads more than two kinesin molecules were binding to a microtubule. All the procedures were done at 25 ± 1 °C.

Nanometry of the stepwise movements

We recorded the bead displacements at a sampling rate of 20 kHz with a bandwidth of 10 kHz. The force of kinesin was calculated from the bead displacement multiplied by the trap stiffness ($0.03\text{--}0.06$ pN nm⁻¹), which was determined from the variance of the thermal fluctuations of a trapped bead with the equipartition theorem of energy¹³. Kinesin displacements were calculated from the bead displacements with an attenuation factor at each force¹³. The average values of the attenuation factor obtained from the thermal fluctuation of the bead between the adjacent stepwise movements¹⁷ were 1.35, 1.10 and 1.06 at 1, 4 and 7 pN, respectively; the attenuation factor was inversely proportional to the load⁸.

The stepwise movements of kinesin were clearly observed after the time record was filtered with a bandwidth of 500 Hz; the noise between the stepwise movements was about 1 nm (the standard deviation over the interval of 10 ms was 1.63, 0.88 and 0.73 nm at 1, 4 and 7 pN, respectively). The step size for the forward and backward movements was obtained directly from the individual stepwise movements and determined as the difference between the average kinesin positions over a 5-ms interval before and after the step.

The dwell time between 8-nm steps at near zero loads was estimated to be about 8 ms on average. This value was obtained by dividing the sliding velocity (960 nm s⁻¹) by the step size (8 nm). Therefore, submillisecond resolution is required for detecting the individual stepwise movements. The temporal resolution for the experimental system was checked from the response time of the force generation of kinesin-coated bead¹⁷. This temporal resolution was essentially retained after passing through the filter. This was confirmed by the absence of any large steps >16 nm (ref. 15) in the raw traces (Figs 1 and 3) and histograms of the step size (Fig. 2a). Thus, our experimental system was equipped with a spatial and temporal resolution that was sufficient to detect all stepwise movements in the time courses studied.

Dwell time

The dwell times between the adjacent stepwise movements were classified into three groups: an 8 nm step at the end phase of the dwell time, a back step (<30 nm), and a detachment (>30 nm). The dwell time was measured as the time from the midpoint of a stepwise movement to that of the next in the bead traces passed through a low-pass filter with a bandwidth of 500 Hz. The dwell time for the 8-nm step had a distribution with a peak at high resolution. Thus, the average dwell time was obtained by integrating the histogram of the dwell time and fitting it to the two-step reaction equation by least squares⁸.

The average dwell time at 0 pN was estimated from the step size (8 nm) divided by the sliding velocity without the optical trap. The sliding velocity of kinesin was measured from the image analysis of bead image²⁷ at ATP concentrations between 1 and 1,000 μM. At very low ATP concentrations, an ATP regenerating system (1 mM phosphoenolpyruvic acid and 10 unit/ml phosphoenolpyruvate carboxylase, final concentrations) was added to the solution. The relationship between the velocity and ATP concentration was fitted to the Michaelis–Menten kinetics equation with $K_m = 36 \pm 3$ μM and $V_{max} = 960 \pm 50$ nm s⁻¹, consistent with previous studies^{8,11}.

ATP turnover time

According to novel Michaelis–Menten kinetics, the sliding velocity of the motor molecules, V , is described as

$$V = \frac{V_{max} \cdot [ATP]}{[ATP] + K_m} \quad (4)$$

where V_{max} is the sliding velocity at saturating concentrations of ATP and K_m is the Michaelis

constant^{10,11}. In consideration of the stepwise movement of kinesin molecules, the microscopic velocity was defined as the step size (8 nm) divided by the dwell time, τ , between adjacent steps. Thus, the equation (4) can be described as

$$\frac{g}{\tau} = \frac{g}{\tau_{cat}} \left(\frac{[ATP]}{[ATP] + K_m} \right) \quad (5)$$

where τ_{cat} is the ATP turnover time and this corresponds to the dwell time at saturating concentrations of ATP. The ATP turnover time was calculated from

$$\tau_{cat} = \tau \left(1 + \frac{K_m}{[ATP]_{limit}} \right) \quad (6)$$

The dwell times in the presence of saturating ($\gg K_m$) and limiting ($< K_m$) ATP are represented for τ_{cat} and τ_{limit} , respectively. The ratio of τ_{limit} to τ_{cat} was calculated as follows

$$\tau_{limit} / \tau_{cat} = \left(1 + \frac{K_m}{[ATP]_{limit}} \right) \quad (7)$$

If the ratio of the dwell times is not changed by the load, then K_m is independent of the load.

RECEIVED 22 FEBRUARY 2002; REVISED 8 JULY 2002; ACCEPTED 27 AUGUST 2002;
PUBLISHED 23 SEPTEMBER 2002.

- Vale, R. D., Reese, T. S. & Sheetz, M. P. Identification of a novel force-generating protein, kinesin, involved in microtubule-based motility. *Cell* **42**, 39–50 (1985).
- Howard, J., Hudspeth, A. J. & Vale, R. D. Movement of microtubules by single kinesin molecules. *Nature* **342**, 154–158 (1989).
- Block, S. M., Goldstein, L. S. B. & Schnapp, B. J. Bead movement by single kinesin molecules studied with optical tweezers. *Nature* **348**, 348–352 (1990).
- Hackney, D. D. Highly processive microtubule-stimulated ATP hydrolysis by dimeric kinesin head domains. *Nature* **377**, 448–450 (1995).
- Vale, R. D. *et al.* Direct observation of single kinesin molecules moving along microtubules. *Nature* **380**, 451–453 (1996).
- Svoboda, K., Schmidt, C. F., Schnapp, B. J. & Block, S. M. Direct observation of kinesin stepping by optical trapping interferometry. *Nature* **365**, 721–727 (1993).
- Coppin, C. M., Finer, J. T., Spudich, J. A. & Vale, R. D. Detection of sub-8-nm movements of kinesin by high-resolution optical-trap microscopy. *Proc. Natl Acad. Sci. USA* **93**, 1913–1917 (1996).
- Higuchi, H., Muto, E., Inoue, Y. & Yanagida, T. Kinetics of force generation by single kinesin molecules activated by laser photolysis of caged ATP. *Proc. Natl Acad. Sci. USA* **94**, 4395–4400 (1997).
- Hua, W., Young, E. C., Fleming, M. L. & Gelles, J. Coupling of kinesin steps to ATP hydrolysis. *Nature* **388**, 390–393 (1997).
- Svoboda, K. & Block, S. M. Force and velocity measured for single kinesin molecules. *Cell* **77**, 773–784 (1994).
- Meyhöfer, E. & Howard, J. The force generated by a single kinesin molecule against an elastic load. *Proc. Natl Acad. Sci. USA* **92**, 574–578 (1995).
- Coppin, C. M., Pierce, D. W., Hsu, L. & Vale, R. D. The load dependence of kinesin's mechanical cycle. *Proc. Natl Acad. Sci. USA* **94**, 8539–8544 (1997).
- Kojima, H., Muto, E., Higuchi, H. & Yanagida, T. Mechanics of single kinesin molecules measured by optical trapping nanometry. *Biophys. J.* **73**, 2012–2022 (1997).
- Kawaguchi, K. & Ishiwata, S. Temperature dependence of force, velocity, and processivity of single kinesin molecules. *Biochem. Biophys. Res. Commun.* **272**, 895–899 (2000).
- Visscher, K., Schnitzer, M. J. & Block, S. M. Single kinesin molecules studied with a molecular force clamp. *Nature* **400**, 184–189 (1999).
- Schnitzer, M. J., Visscher, K. & Block, S. M. Force production by single kinesin motors. *Nature Cell Biol.* **2**, 718–723 (2000).
- Nishiyama, M., Muto, E., Inoue, Y., Yanagida, T. & Higuchi, H. Substeps within the 8-nm step of the ATPase cycle of single kinesin molecules. *Nature Cell Biol.* **3**, 425–428 (2001).
- Howard, J. *Mechanics of Motor Proteins and the Cytoskeleton* (Sinauer Associates, Sunderland, MA, 2001).
- Fisher, M. E. & Kolomeisky, A. B. Simple mechanochemistry describes the dynamics of kinesin molecules. *Proc. Natl Acad. Sci. USA* **98**, 7748–7753 (2001).
- Veigel, C. *et al.* The motor protein myosin-1 produces its working stroke in two steps. *Nature* **398**, 530–533 (1999).
- Wang, M. D. *et al.* Force and velocity measured for single molecules of RNA polymerase. *Science* **282**, 902–907 (1998).
- Mehta, A. D. *et al.* Myosin-V is a processive actin-based motor. *Nature* **400**, 590–593 (1999).
- Gilbert, S. P., Webb, M. R., Brune, M. & Johnson, K. A. Pathway of processive ATP hydrolysis by kinesin. *Nature* **373**, 671–676 (1995).
- Ma, Y. Z. & Taylor, E. W. Mechanism of microtubule kinesin ATPase. *Biochemistry* **34**, 13242–13251 (1995).
- Schnitzer, M. J. & Block, S. M. Kinesin hydrolyses one ATP per 8-nm step. *Nature* **388**, 386–390 (1997).
- Rief, M. *et al.* Myosin-V stepping kinetics: a molecular model for processivity. *Proc. Natl Acad. Sci. USA* **97**, 9482–9486 (2000).

27. Woledge, R. C., Curtin, N. A. & Homsher, E. *Energetic Aspects of Muscle Contraction* 167–275 (Academic, London, 1985).
28. Tomishige, M. & Vale, R. D. Controlling kinesin by reversible disulfide cross-linking: identifying the motility-producing conformational change. *J. Cell Biol.* **151**, 1081–1092 (2000).
29. Hirose, K., Lockhart, A., Cross, R. A. & Amos, L. A. Three-dimensional cryoelectron microscopy of dimeric kinesin and ncd motor domains on microtubules. *Proc. Natl Acad. Sci. USA* **93**, 9539–9544 (1996).
30. Kawaguchi, K. & Ishiwata, S. Nucleotide-dependent single- to double-headed binding of kinesin. *Science* **291**, 667–669 (2001).
31. Rice, S. *et al.* A structural change in the kinesin motor protein that drives motility. *Nature* **402**, 778–784 (1999).
32. Kikkawa, M. *et al.* Switch-based mechanism of kinesin motors. *Nature* **411**, 439–445 (2001).
33. Romberg, L. & Vale, R. D. Chemomechanical cycle of kinesin differs from that of myosin. *Nature* **361**, 168–170 (1993).
34. Sosa, H., Peterman, E. J. G., Moerner, W. E. & Goldstein, L. S. B. ADP-induced rocking of the kinesin motor domain revealed by single-molecule fluorescence polarization microscopy. *Nature. Struct. Biol.* **8**, 540–544 (2001).
35. Kitamura, K., Tokunaga, M., Iwane, A. H. & Yanagida, T. A single myosin head moves along an actin filament with regular steps of 5.3 nanometres. *Nature* **397**, 129–134 (1999).
36. Vale, R. D. & Milligan, R. A. The way things move: looking under the hood of molecular motor proteins. *Science* **288**, 88–95 (2000).
37. Inoue, Y., Iwane, A. H., Miyai, T., Muto, E. & Yanagida, T. Motility of single one-headed kinesin molecules along microtubules. *Biophys. J.* **81**, 2838–2850 (2001).
38. Okada, Y. & Hirokawa, N. Mechanism of the single-headed processivity: diffusional anchoring between the K-loop of kinesin and the C terminus of tubulin. *Proc. Natl Acad. Sci. USA* **97**, 640–645 (2000).
39. Rogers, K. R. *et al.* KIF1D is a fast non-processive kinesin that demonstrates novel K-loop-dependent mechanochemistry. *EMBO J.* **20**, 5101–5113 (2001).
40. Tucker, C. & Goldstein, L. S. B. Probing the kinesin-microtubule interaction. *J. Biol. Chem.* **272**, 9481–9488 (1997).
41. Nogales, E., Wolf, S. G. & Downing, K. H. Structure of the $\alpha\beta$ tubulin dimer by electron crystallography. *Nature* **391**, 199–203 (1998).
42. Feynman, R. P. in *The Feynman Lectures on Physics* Vol. I (eds Feynman, R. P., Leighton, R. B. & Sands, M. L.) (Addison-Wesley, Reading, MA, 1963).
43. Oosawa, F. Sliding of actin filament on myosin and a flexible ratchet. *Jikeikai. Med. J.* **36**, 219–231 (1989).
44. Vale, R. D. & Oosawa, F. Protein motors and Maxwell's demons: does mechanochemical transduction involve a thermal ratchet? *Adv. Biophys.* **26**, 97–134 (1990).
45. Hirakawa, E., Higuchi, H. & Toyoshima, Y. Y. Processive movement of single 22S dynein molecules occurs only at low ATP concentrations. *Proc. Natl Acad. Sci. USA* **97**, 2533–2537 (2000).
46. Kojima, H., Kikumoto, M., Sakakibara, H. & Oiwa, K. Mechanical properties of single-headed processive motor, inner-arm dynein subspecies-c of *Chlamydomonas* studied at the single molecule level. *J. Biol. Phys.* (in the press).

ACKNOWLEDGEMENTS

We thank Y. Ishii, F. Oosawa, Y. Inoue and colleagues of Single Molecule Processes Project, and Osaka University for discussions; J. West, E. Muto, H. Kojima and Y. Taniguchi for critically reading the manuscript. This work was partially supported by JSPS Research Fellowships for Young Scientists (M.N.). Correspondence and requests for materials should be addressed to H.H.

COMPETING FINANCIAL INTERESTS

The authors declare that they have no competing financial interests.